DOI: 10.1002/cbic.201000497

Induction of Cell–Cell Connections by Using in situ Laser Lithography on a Perfluoroalkyl-Coated Cultivation Platform

Kazunori Okano,*[a, b] David Yu,[c] Ai Matsui,[a] Yasuyo Maezawa,[a] Yoichiroh Hosokawa,[a] Atsushi Kira,[d] Mie Matsubara,[a] Ian Liau,[c] Hiroshi Tsubokawa,[b] and Hiroshi Masuhara[a, c]

This article describes a novel laser-directed microfabrication method carried out in aqueous solution for the organization of cell networks on a platform. A femtosecond (fs) laser was applied to a platform culturing PC12, HeLa, or normal human astrocyte (NHA) cells to manipulate them and to facilitate mutual connections. By applying an fs-laser-induced impulsive force, cells were detached from their original location on the plate, and translocated onto microfabricated cell-adhesive domains that were surrounded with a cell-repellent perfluoroalkyl (R_f) polymer. Then the fs-laser pulse-train was applied to the R_f polymer surface to modify the cell-repellent surface, and to make cell-adhesive channels of several μm in width between each cell-adhesive domain. PC12 cells elongated along the channels and made contact with others cells. HeLa and NHA cells also migrated along the channels and connected to the other cells. Surface analysis by X-ray photoelectron spectroscopy (XPS) and atomic force microscopy (AFM) confirmed that the R_f polymer was partially decomposed. The method presented here could contribute not only to the study of developing networks of neuronal, glial, and capillary cells, but also to the quantitative analysis of nerve function.

Introduction

Cell culturing is one of the fundamental techniques in many biological studies including clinical examinations. The fabrication and usage of artificially organized cell-networks on a micro cell-culture platform has been reported; this is going to be an essential strategy for obtaining precise information on cells.[1,2]

In order to construct the cell networks, several technologies are required: specific domains for cell adhesion need to be arranged on a solid platform, cells must be translocated individually and attached onto the domains, and the connections between the arrayed cells are important to make functional cell networks. Cell-adhesive domains have been fabricated by applying dry and wet lithography,[3–5] laser processing of soft materials,[6] microstamping,[7–10] and ink-jet printing.[11,12] When constructing a cell network, a reliable cell-array platform is required for long-term cultivation. Our research group has proposed the use of a new platform with micro cell-adhesion domains surrounded by high-molecular-mass R_f residues (M_r 5000–7000) that prevent protein adsorption and cell adhesion.[13] Quartz crystal microbalance (QCM) measurements of the surface have confirmed the inhibition of protein adsorption, and the surface was water- and oil-repellent, as confirmed from contact-angle analysis. Considering these results, the R_f surface prevents adsorption of extradomain matrix proteins, and consequently the region is cell-repellent.[13] Our platform is biochemically stable and autoclavable.

Although cells successfully grew on the cell-adhesive domains, it seems inadequate simply to make a cell-network platform where different kinds of cells are arranged. In living organisms, cells divide, differentiate, and migrate to fulfill their functions. It is sometimes necessary to alter the prepared platform patterns dynamically to permit cell–cell interactions while cells are growing. Several studies have investigated the dynamic control of cell adhesivity on solid surfaces.[6,14–18] Studies that demonstrated the switching of surface cell-adhesive characteristics and cell-releasing states relied on the use of electrochemically reactive,[14,15] photoactive,[16] enzymatically reactive,[17] and thermally responsive polymers.[18] Agarose is effective for preventing cell adhesion. Agarose, coated on glass that had a thin chromium layer (acting as a photothermal transducer), was locally removed by IR-laser irradiation under aqueous conditions.[6] As for the spatial resolution of patterning, direct laser application, which permits the changing of platform pat-

[a] Dr. K. Okano, A. Matsui, Y. Maezawa, Prof. Dr. Y. Hosokawa, M. Matsubara, Prof. Dr. H. Masuhara
Graduate School of Materials Science
Nara Institute of Science and Technology
8916-5 Takayama, Ikoma, Nara 630-0192 (Japan)
E-mail: okano@ms.naist.jp

[b] Dr. K. Okano, Prof. Dr. H. Tsubokawa
Kansei Fukushi Research Center, Tohoku Fukushi University
6-149-1 Kunimigaoka, Aoba-ku, Sendai 989-3201 (Japan)
Fax: (+81) 22-728-6040
E-mail: okano-k@tfu-mail.tfu.ac.jp

[c] D. Yu, Prof. Dr. I. Liau, Prof. Dr. H. Masuhara
Department of Applied Chemistry and Institute of Molecular Science
National Chiao Tung University
1001 Ta Hsueh Road, Hsinchu 30010 (Taiwan)

[d] Dr. A. Kira
Research and development division, ULVAC Inc.
2500 Hagizono, Chigasaki, Kanagawa 253-8543 (Japan)

terns, might be the best choice for the dynamic control of cell networks.

In this paper, we describe newly developed cell-manipulation methods, and in situ laser lithographic techniques that apply femtosecond laser pulses as a fundamental technology for constructing cell networks. We demonstrated that individual cells can be successfully arrayed on target microfabricated cell-adhesive domains on a platform, and that the cells then connect with each other. All these processes are completed during a series of culturing stages in medium.

Results

Application of fs laser in cell arraying and in situ lithography

We employed two characteristics of fs laser technology for making cell networks on an R_f platform, as shown in Figure 1.

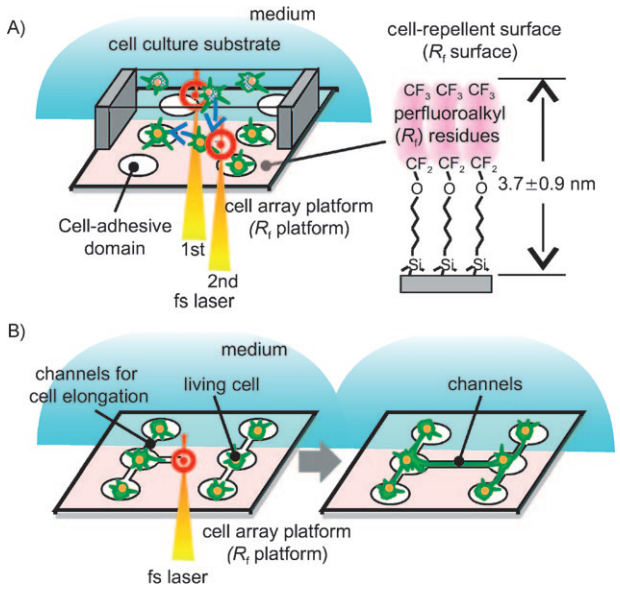

Figure 1. Schematic representation of our method for organizing cell networks on the platform. A) Cell preparation on cell-array platform; B) modification of platform patterns during cell culture.

When a single pulse from an intense fs laser is applied to an aqueous solution, a shockwave and a cavitation bubble are generated at the focal point. Following expansion and collapse of the bubble, the convection front propagates from the focal point into the surrounding area as a stress wave.[19] The resulting stress wave affects a cell-adhesive area to a diameter of several tens of μm, so it serves as a tool for living-cell manipulation that is locally and temporally controllable. Our group has demonstrated that the stress wave could detach cells individually from a culture substrate.[19–21] Since the force affecting the cells was estimated to be of the order of just nano-Newtons,[19] cells (e.g., mouse embryonic NIH3T3) would readhere to the substrate in high yield (80%).[20] This value is comparable to, or higher than, that for cells released by trypsin.[21] In this study, we showed that detached cells are sequentially translocated to adjacent cell-adhesive domains on the R_f platform in a few minutes by applying the stress wave as illustrated in Figure 1A.

When the fs laser is focused on the platform, the glass absorbs the photons, and this is followed within a short time by an ablation sequence. Since the fs-laser pulses are short, the ablation is not photothermal destruction.[22,23] We applied this non-photothermal phenomenon to modify the platform surface (Figure 1B). To make channels for cell-to-cell connections on the platform, an intense fs-laser pulse-train (800 nm, 130 fs, 0.5–1.8 μJ per pulse, 1 kHz) was focused on the R_f polymer layer during the cell culture process. This treatment modifies the R_f polymer surface to create a cell-adhesive region, so that cells can elongate or migrate across the modified area, which facilitates the formation of mutual connections.

We estimated the area affected by the laser-induced stress-wave on the cell array-stage (Figure 1A); the experimental design is shown in Figure 2A. A single fs-laser pulse was applied to glass covered with monolayer microparticles (2 μm diameter), and the focal point was adjustable from a position 100 μm from the glass surface (within the liquid) to −30 μm (within the glass). The area over which microparticles detached was monitored by a laser-scattering microscope (see Figure 2B): microparticles were clearly detached near the laser focal point. The diameter of the detached area was plotted against the focal depth (Figure 2C), from which it was concluded

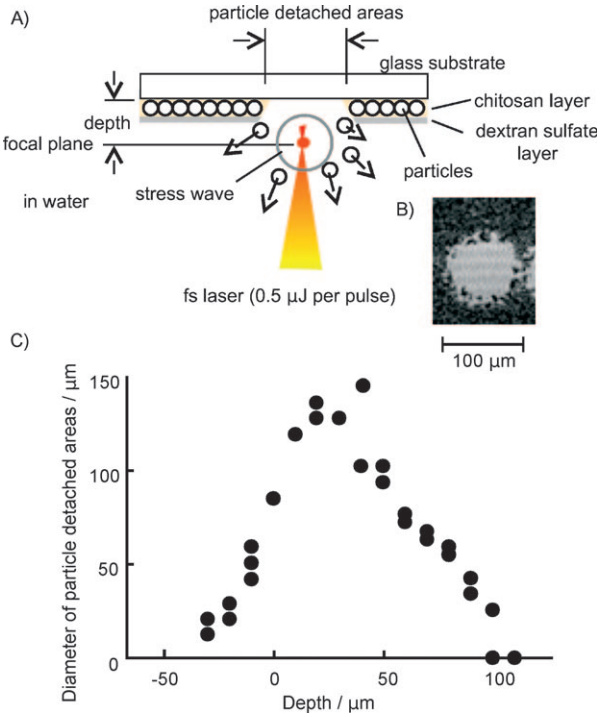

Figure 2. Estimation of the affected area resulting from the fs-laser-induced stress-wave. A) Schematic diagram of microparticles released from the glass surface; B) typical scattering image of microparticle detached area when the fs laser was focused in water at 50 μm depth from the glass surface; C) microparticle detached area vs. depth relationship obtained by single pulse fs-laser irradiation.

ed that particles were more efficiently removed when the laser focus was located in the aqueous solution than in the glass. The best position was 20 μm from the glass surface: at 0.8 μJ per pulse the impulsive force reached as far as 70 μm from the focal point. The particle-detached area was reduced drastically when the laser was focused in the glass. A focal point 10–30 μm from the platform (z-axis) and 10–30 μm from the target cell (*x*–*y* plane) is recommended for efficient cell detachment. Although both a stress wave and laser ablation can cause the detachment of particles/cells, we concluded that the former was the dominant, because the laser ablation area resulting from multiphoton adsorption was estimated to be small (3 μm at 0.8 mW laser power).

To examine the condition of the R_f platform surface following application of the fs laser on the in situ laser lithography (Figure 1 B), we analyzed the surface by using atomic force microscopy (AFM). As shown in the scanning image (Figure 3),

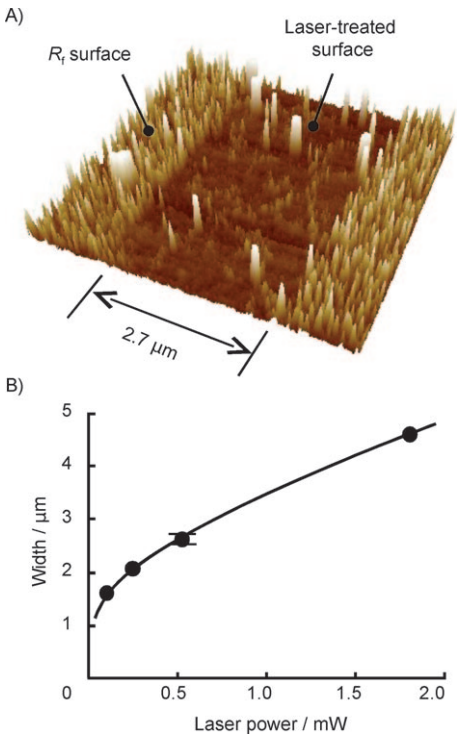

Figure 3. AFM surface-analysis of fs-laser-treated area. A) AFM scanning image of the R_f platform where the 0.5 mW fs laser irradiated. B) The surface-modified area width on the laser scanning conditions, ranging from 0.1 to 1.8 mW. Error bars at 0.5 mW laser powered show standard deviation ($n=3$).

many pillars were observed on the original R_f surface: the density was 18.9 pillars per μm^2, and the height was about 10 nm. The height of the pillars was reduced in the laser-applied area; this indicated that fs laser modified the R_f layer. The effect on the scanned area depended on laser power; the line widened with laser power: 1.6, 2.1, 2.6, and 4.6 μm at 0.10, 0.25, 0.50, and 1.8 mW laser power, respectively (Figure 3 B). The variation in the modified area width was 0.1 μm ($n=3$) at 0.5 mW. As the scanning rate was 20 $\mu m\,s^{-1}$ at 1 kHz, the laser pulses were introduced every 20 nm. Pulses of 80, 103, 130, and 230 irradiated the same place with the laser power at 0.10, 0.25, 0.50, and 1.8 mW, respectively, and the number of pulses was calculated from the width and the scanning rate. When the laser pulse passed across the R_f surface at 0.1 mW, debris was frequently observed on the laser-treated area; it appeared that R_f material had melted and reattached to the laser-scanned surface (data not shown). Therefore, this method can modify the R_f surface with a width as narrow as 2 μm in aqueous solution, when carried out with an fs-laser power of 0.25 mW. The scanning rate could be increased to 80 $\mu m\,s^{-1}$ at 1 mW power for successful modification.

We also analyzed the changes in the chemical elements at the surface by using X-ray photoelectron spectroscopy (XPS; Figure 4). The XPS energy spectra indicated that the fluorine

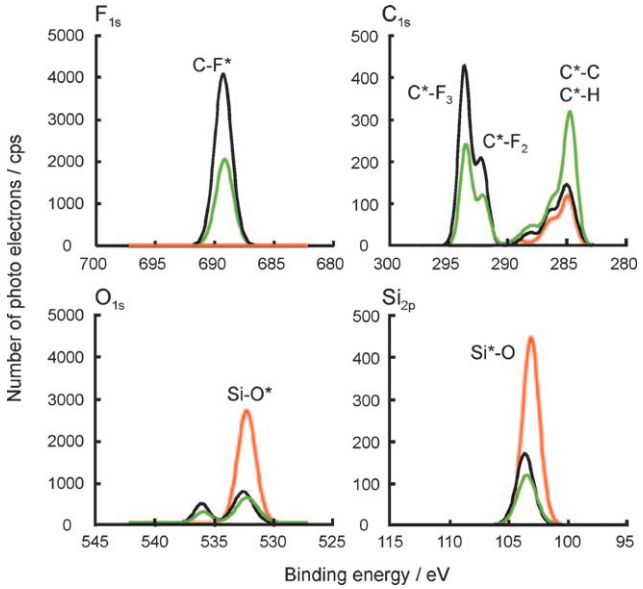

Figure 4. XPS surface analysis: energy spectra of fluorine (F_{1s}), carbon (C_{1s}), oxygen (O_{1s}), and silicate (Si_{2p}). Black, green, and red spectra were obtained from intact R_f surface, fs-laser-treated R_f surface, and bare glass surfaces, respectively.

level at the R_f surface (binding energy: 689.2 eV) decreased to 46% in the laser-treated area. C_{1s} signals from CF_3 and CF_2 (detected at 293.6 and 292.2 eV, respectively) also decreased to 44 and 50%, respectively, while C_{1s} signals from hydrocarbon groups (284.8 eV, typically C–C, C–H) increased to 158%. Therefore, the R_f layer was modified and the fluorine residue was partially removed. It was concluded that the carbon skeletal frame remained (hydrocarbon or graphite), as the 284.8 eV signals increased in the laser-treated area. Signal intensities for silicate and oxygen at the R_f layer were small compared to that for bare glass, but did not recover in the laser-treated area. All the data showed that the laser-treated surface was covered with degraded R_f material (e.g., hydrocarbon or graphite).

Induction of cell–cell connections on the platform

Figure 5 shows a typical procedure for cell arrangement, in which individual PC12 cells are detached from the lower surface of the cell culture substrate (Figure 5 Aand B), and translocated to the platform (Figure 5 C). When the fs laser was applied with the focal point (cross, in Figure 5 A) 10–30 μm away from the cell (arrow), the targeted cell became detached from the culture plate (Figure 5 B). The cell then dropped onto the platform (Figure 5 C) within 1 min (sedimentation rate ca. 50 μm min^{-1}). Neighboring cells on the culture plate did not detach, even after four days. On the platform, the cell divided into two daughter cells every two days (Figure 5 D). The doubling time was the same as that for intact PC12 cells. These results suggest that the fs laser can detach specific cells without affecting basic functions, such as cell division.

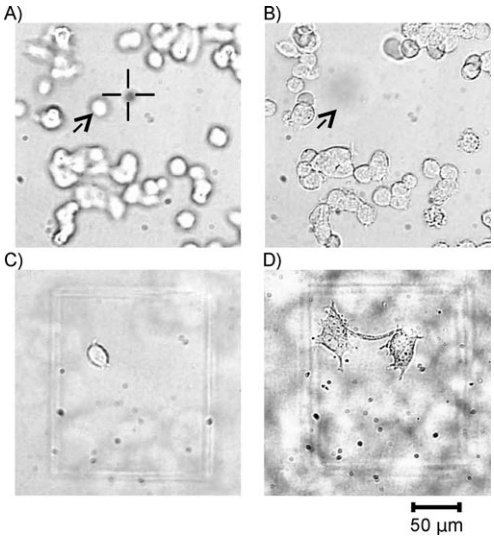

Figure 5. Micrographs showing cell detachment by fs-laser-induced stress-wave. A) and B) Cells on the upper cell-culture plate (Figure 1 A), which were obtained immediately, and 30 min after the fs-laser pulse irradiation to the cross point, respectively. Arrows indicate the target cell. C) and D) Cells transferred to the platform at 30 min, and two days after the laser irradiation, respectively.

As a next step, we applied the fs laser to move cells toward the cell-adhesive domain, and successfully arranged the cells on the platform as shown in Figure 6 A–C. Such cell-transportation was sensitive to the distance between the laser focal point and the cell. The laser application sometimes caused hypertrophy of the cells, and an increase in the permeability of the cell membrane when the focal point was too close to the cell ($\leq$10 μm). High-power laser pulses ($\geq$1.5 μJ per pulse) also damaged the cells even when the distance was greater than 10 μm. Therefore, in this procedure we ensured that the distance between the laser focal point and the cell was greater than 10 μm, and that the laser power was less than 1.0 μJ per pulse.

To make channels for promoting cell-to-cell junctions on the platform, the fs laser was focused in the glass near the R_f layer,

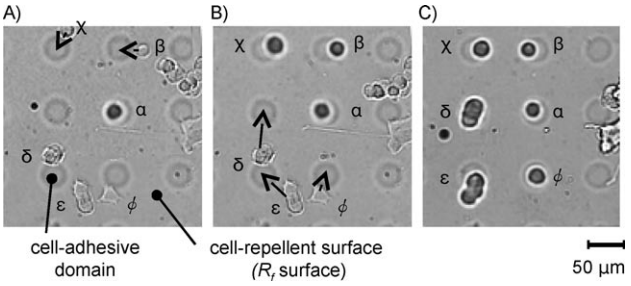

Figure 6. Micrographs of cell translocations by fs-laser-induced stress-wave. A) All cells except α were adhered to the culture plate, while α was located at a cell-adhesive domain of the platform. B) Cells β and χ were translocated; cells δ, ε, and ϕ still adhered to the cell culture plate. C) All cells were translocated on to cell-adhesive domains. Arrows indicate directions of cell transportation after the cells descended from the culture plate. As the focal plane in the micrographs was at the cell culture plate, focused and defocused cells are assigned to the cell-culture plate and the cell-array platform, respectively.

leading to modification of the pattern. Figure 7 A demonstrates the process of making a channel between cell adhesion domains, where PC12 cells were already attached. Luminescence was detected at the laser focus, and visible lines appeared on the R_f platform in the laser-scanned areas. The cells never moved on or detached from the platform during this lithographic process.

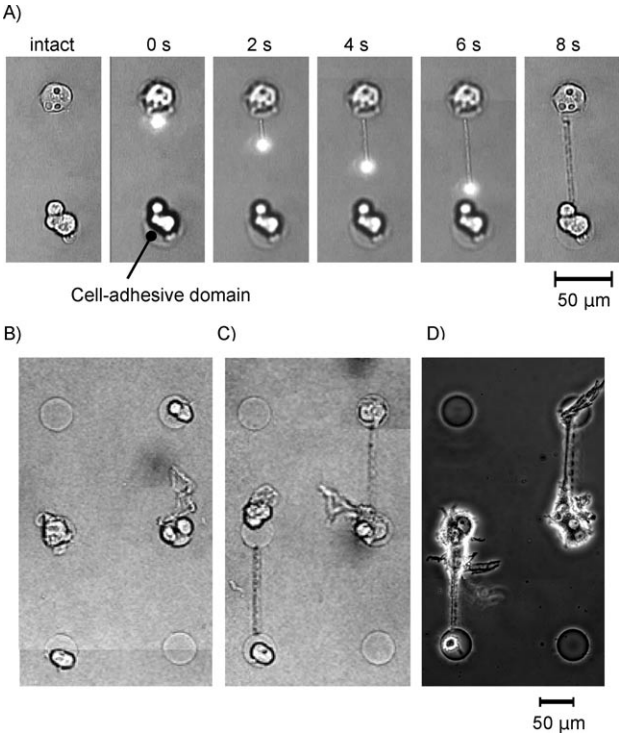

Figure 7. Channel preparation for promoting PC12 cell junctions: A) Time-lapse images of the R_f platform through the in-situ lithography process. The focused fs-laser beam scanned the inside of the platform near the surface between areas where the cells were already adhered. B), C), and D) Cells on the platform before laser treatment, after channel preparation, and after four days of cell culture after the channel preparation, respectively.

Following channel preparation by this lithographic method, PC12 cells on the platform were continuously cultured in medium containing nerve growth factor (NGF, a protein that induces PC12 differentiation) for one week. The PC12 differentiated, elongated along the channel, and attached to one another within four days (Figure 7B–D). PC12 cells remained at cell-adhesive domains and channels, and did not migrate to the R_f area or vacant cell-adhesive domains. Although there was some growth into the R_f area, this never adhered to the R_f surface. These results suggest that the in situ lithographic method is useful for making artificial connections between identical cells.

Figure 8 shows the result obtained for a platform on which HeLa cells were arrayed. After cells were cultured for 16 h on cell-adhesive domains, the R_f layer between the adhered cells was modified to form channels of 2.6 or 10 μm width. The

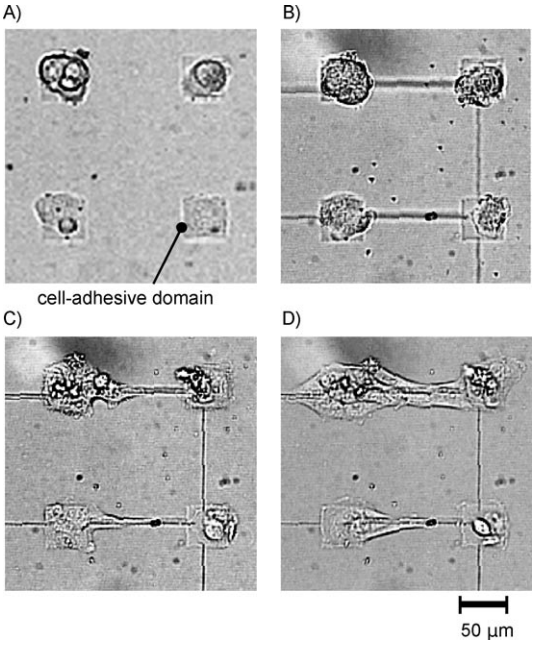

Figure 8. Cell organization after creating channels between HeLa cells: Micrographs were taken A) when the platform was intact, B) just after making channels, C) after 4.5 h, and D) after 9 h incubation.

laser pulse train (0.8 mW, 1 kHz) was focused under the R_f layer, and scanned several times at 2 μm pitch to make lines of the required widths. The HeLa cells elongated along the 10 μm channels and attached to each another within 8 h (100 μm between cell-adhesive domains). In this case, the cell-extension rate was estimated to be 7–10 $\mu m\,h^{-1}$. The HeLa cells looked for footholds on the wider channels and elongated along the direction of channels, but did not elongate through the 2 μm-wide channels.

In situ laser lithography can modify different types of cell-repellent material, for example a copolymer of 2-methacryloyloxyethylphosphorylcholine (MPC), which is often used to prohibit protein, DNA, and cell adsorption onto solid surfaces. Figure 9 shows NHA migration on a modified cell-array plat-

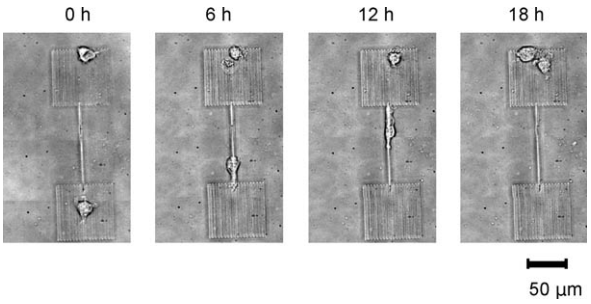

Figure 9. Time-lapse images of cell migration along a fabricated channel. The cell-repellent area surrounding the cell adhesive domains were coated with MPC polymer. The cell sample was NHA.

form, in which the cell-repellent area was covered by MPC polymer. The square areas (70×70 μm) were drawn by our in situ laser lithographic method. When NHA cells were spread on the platform, cells adhered only on the square area. When a channel was prepared between two cell-adhesive domains, the NHA cell on one domain migrated along the fabricated channels toward the other domain, and finally the two cells interacted.

Discussion

The applicability of laser-induced cell-detachment depended on both laser power and cell species. The PC12 cell detachment phenomenon was observed at laser powers higher than 0.1 μJ per pulse, but multiple cells were sometimes detached at powers higher than 1.0 μJ per pulse. Additionally, the glass surface was frequently damaged (engraved) by stress waves when the pulse-energy was above 1.5 μJ, and the laser was focused near the surface of the culture plate. We typically used between 0.5 and 1.0 μJ per pulse to detach cells from the culture plate. As PC12 adhesion was weak, the cells were easily detached from the surface by applying one to three laser pulses. The neuron-like cells induced from PC12 cells, required additional irradiation pulses to detach. HeLa and NHA cells that clung strongly to the culture substrate-surfaces through extracellular matrix required three to ten pulses to be detached.

We showed that lithography by using an fs laser was effective in aqueous solution, for example, water and cell-culture medium; the laser-treated surface became hydrophilic. Although visible lines appeared in the laser-treated areas on the platform, the glass surface was not engraved; only the R_f layer was modified by the focused fs laser. AFM surface-analysis showed pillars on the R_f surface of about 10 nm. By using ellipsometry measurement, the thickness of the R_f layer on the glass surface had previously been shown to be 3.7 ± 0.9 nm.[13] The difference between these values is probably attributable to a characteristic of the AFM method (strongly influenced by the surface material). The R_f surface is well known to have low surface energy,[24] so it had reduced interactions with the AFM probe, and thus give such a higher value for thickness.

XPS analysis shows that fluorine had been removed for the fs-laser-treated surface, but that the amount of carbon had in-

creased. There is a possibility that the R_f residue reacted chemically or photothermally, and released the fluorine compounds, and that this resulted in the surface becoming carbonized (the C−C XPS spectrum at 284.8 eV increased in the laser-treated area). Consequently, cells could adhere to the places where the covalently immobilized R_f layer on the platform had become degraded, and a carbonized surface was exposed. It is possible that the fluorine element was partially released because it has a wide collision cross-section to electromagnetic waves and X-rays.[24]

Conclusions

We have demonstrated a fundamental method for arraying living cells; this enables the creation of artificial cell–cell connections on demand. The fs laser facilitated the detachment of cells from the culture plate to another platform, as well as modification of the platform patterns to direct cell growth. An excellent feature of our fs-laser lithographic method is that all processes can be performed in situ in aqueous solution. This is an invaluable property for biological applications of microdevice technologies that use living cells. The method to modify the platform pattern can be applied ubiquitously because it does not depend on the platform material: another beneficial aspect.

Our results show that the fs laser is a powerful tool for developing platform-type devices for living cells, and that it will contribute to the development of networks consisting of neuronal, glial, and capillary cells, etc. This technology will be useful for many disciplines that study nerve function, as well as clinical chemistry, including the discovery of new drugs.

Experimental Section

Materials: The cell-array platform used here was specially developed by ULVAC, Inc. (Chigasaki, Japan). MPC polymer (Lipidure-CM5206) was kindly given by the NOF Corporation (Tokyo, Japan). Glass plates (12×2×0.4 mm) for cell culture were ordered from Matsunami Glass Ind., Ltd. (Kishiwada, Japan). Glass-based dishes and cell culture plasticware were purchased from Asahi Glass Co. (Funabashi, Japan). PC12 (RCB0009) and HeLa (RCB0007) cells were provided by the RIKEN CELL BANK (Tsukuba, Japan). Human normal astrocyte (CC-2565) and its medium kit with growth supplements (CC-3186) were obtained from Lonza Inc. (Walkersville, MD, USA). Dulbecco's modified eagle medium (DMEM), fetal bovine serum (FBS), horse serum (HS), and mixed antibiotics solution of streptomycin/ penicillin were purchased from GIBCO/Invitrogen. The collagen used here was Cellmatrix type 1C (Nitta Gelatin Inc., Osaka, Japan). All chemicals were analytical grade.

System: A regenerative, amplified Hurricane fs-laser (SpectraPhysics, Mountain View, CA; Ti:sapphire, 800 nm, 1000 Hz) was connected to an IX71 inverted microscope (Olympus) with a shutter, ND filter, and object lens (×20, Olympus, N.D. 0.46). In order to culture the cells for a long time, the microscope was equipped with a BIOS-102T PC-controlled automatic XY-stage (Sigmakoki Co., Tokyo, Japan) and a micro CO_2 incubator system (MI-IBC, Olympus). Cells were observed with an ICD-878 analogue CCD camera (Ikegami Tsushinki Co., Tokyo, Japan) and a Fluoview 300 laser scattering imaging system (Olympus).

Preparation of a cell array: Cell culture substrate (glass plate, 12×2×0.4 mm) was cleaned with atmospheric plasma by using an A1000 bench-top plasma generator (Sakigake Semiconductor Co., Ltd., Kyoto, Japan). Silicon rubber spacers (2×2×0.1 mm) were placed at both ends of the plates. Prior to cell seeding, the cell culture plates were coated with collagen in HCl solution (1 mM, pH 3) for 10 min. The plates were rinsed with sodium phosphate buffer (50 mM, pH 7.4). PC12 cells were seeded onto the substrates right-side up (spacer side) at a density of 40 cells per mm^2. PC12 cells on the substrates were cultured in DMEM supplemented with 10% FBS, 10% HS, streptomycin (100 $\mu g\,mL^{-1}$), and penicillin (100 $U\,mL^{-1}$) at 37 °C under an atmosphere of 90% relative humidity and 5% CO_2. HeLa cells were cultured on the substrate and under the same condition except for the absence of HS. NHA cells were cultured following the supplier instructions (Lonza). The cultured cell-substrate was placed (upside-down) 100 μm above the platform, and placed in a 35 mm diameter glass dish filled with culture medium (3 mL). The cells were hung above the platform in this state. The fs-laser pulses (single to several pulses, 0.5–1.0 μJ per pulse) were focused in the medium at about 20 μm from the surface of the cultured cell substrate to detach the cells. Additionally, the fs-laser pulses were focused near the detached cells to transport them along the predetermined cell adhesive domains on the cell-array platform. To prevent photochemical and photothermal effects on the cell, the laser pulse was aimed carefully around the cell, not directly on it. After cells re-adhered to the platform, they were cultured as described above.

Modification of cell-repellent surface by in situ laser lithography: After cell arrangement, the fs laser (800 nm, 1 kHz, 0.5–1.8 mW) was focused on the cell-array platform. We drew lines on the cell-repellent surface at 20 $\mu m\,s^{-1}$ with the fs laser, between the cell adhesive domains. Following that, the cells on the platform were continuously cultured and monitored at 30 min intervals until the cells contacted completely. Cells were cultured as described above, but with NGF supplement (50 $ng\,mL^{-1}$) in PC12 culture medium.

Analysis of the fs-laser-modified surface: AFM scanning images were taken on a Bioscope SZ (Veeco, USA) in tapping mode at 300 kHz with an OMCL-AC160TS cantilever and a silicon nitride tip (spring constant: 42 $N\,m^{-1}$). Chemical species formed on the fs-laser-modified surface were identified with an AXIS 165 XPS Spectrometer (Kratos, Manchester, UK) using monochromatic Al radiation (1486.6 eV; pass energy: 40 eV). The XPS analysis was carried out within a short time to reduce the degradation of R_f residue to 5–10% during X-ray irradiation. The signals were resolved by using a Gaussian-Lorenzian peak model, and corrected for the binding energy of C_{1s} (284.8 eV for hydrocarbon groups).[25] Surface compositions were estimated by using the National Institute of Standards and Technology (NIST) XPS-Database.[25]

Acknowledgements

This study was funded in part by a Grant-in-Aid for Science Research, Scientific Research (B) (No.20310075) to K.O., a Grant-in-Aid for Young Scientists (A) (No.1986007) to Y.H. from the Japan Society for the Promotion of Science (JSPS), and a Grant-in-Aid on Priority Area "Bio Manipulation" (No.20034061) to H.M. from the Ministry of Education, Culture, Sports, Science and Technology (MEXT) of Japan. This study was also supported by the Program of Funding Basic Research Centers in Private Universities (MEXT)

to the Kansei Fukushi Research Center, Tohoku Fukushi University (2009). H.M. also thanks the MOE-ATU Project (Nat. Chiao Tung Univ.) sponsored by the Ministry of Education Taiwan, and the National Science Council Taiwan (0970027441) for their support. We also thank Dr. Akio Hayashi of the NOF Corporation for his kind gift of MPC polymer.

Keywords: artificial cell networks · cell adhesion · cell arrays · laser chemistry · lithograhy

[1] A. Khademhosseini, K. Y. Suh, J. M. Yang, G. Eng, J. Yeh, S. Levenberg, R. Langer, *Biomaterials* **2004**, *25*, 3583 – 3592.
[2] K. Yasuda, *J. Mol. Recognit.* **2004**, *17*, 186 – 193.
[3] W. He, C. R. Halberstadt, K. E. Gonsalves, *Biomaterials* **2004**, *25*, 2055 – 2063.
[4] D. Kleinfeld, K. H. Kahler, P. E. Hockberger, *J. Neurosci.* **1988**, *8*, 4098 – 4120.
[5] I. Inoue, Y. Wakamoto, H. Moriguchi, K. Okano, K. Yasuda, *Lab Chip* **2001**, *1*, 50 – 55.
[6] H. Moriguchi, Y. Wakamoto, Y. Sugio, K. Takahashi, I. Inoue, K. Yasuda, *Lab Chip* **2002**, *2*, 125 – 130.
[7] S. Zhang, L. Yan, M. Altman, M. Lässle, H. Nugent, F. Frankel, D. A. Lauffenburger, G. M. Whitesides, A. Rich, *Biomaterials* **1999**, *20*, 1213 – 1220.
[8] R. S. Kane, S. Takayama, E. Ostuni, D. E. Ingber, G. M. Whitesides, *Biomaterials* **1999**, *20*, 2363 – 2376.
[9] D. W. Branch, B. C. Wheeler, G. J. Brewer, D. E. Leckband, *IEEE Trans. Biomed. Eng.* **2000**, *47*, 290 – 300.
[10] A. K. Vogt, G. Wrobel, W. Meyer, W. Knoll, A. Offenhäusser, *Biomaterials* **2005**, *26*, 2549 – 2557.
[11] N. E. Sanjana, S. B. Fuller, *J. Neurosci. Methods* **2004**, *136*, 151 – 163.
[12] W. C. Wilson Jr. , T. Boland, *Anatom. Rec. A* **2003**, *272 A*, 491 – 496.
[13] A. Kira, K. Okano, Y. Hosokawa, A. Naito, K. Fuwa, J. Yuyama, H. Masuhara, *Appl. Surf. Sci.* **2009**, *255*, 7647 – 7651.
[14] W.-S. Yeo, M. N. Yousaf, M. Mrksich, *J. Am. Chem. Soc.* **2003**, *125*, 14994 – 14995.
[15] H. Kaji, K. Tsukidate, M. Hashimoto, T. Matsue, M. Nishizawa, *Langmuir* **2005**, *21*, 6966 – 6969.
[16] J. Nakanishi, Y. Kikuchi, T. Takarada, H. Nakayama, K. Yamaguchi, M. Maeda, *J. Am. Chem. Soc.* **2004**, *126*, 16314 – 16315.
[17] S. J. Todd, D. J. Scurr, J. E. Gough, M. R. Alexander, R. V. Ulijn, *Langmuir* **2009**, *25*, 7533 – 7539.
[18] N. Idota, T. Tsukahara, K. Sato, T. Okano, T. Kitamori, *Biomaterials* **2009**, *30*, 2095 – 2101.
[19] Y. Hosokawa, H. Takabayashi, S. Miura, C. Shukunami, Y. Hiraki, H. Masuhara, *Appl. Phys. A* **2004**, *79*, 795 – 798.
[20] T. Kaji, S. Ito, H. Miyasaka, Y. Hosokawa, H. Masuhara, C. Shukunami, Y. Hiraki, *Appl. Phys. Lett.* **2007**, *91*, 023904.
[21] Y. Maezawa, Y. Hosokawa, K. Okano, M. Matsubara, H. Masuhara, *Appl. Phys. A* **2010**; *101*, 129 – 131.
[22] Y. Hosokawa, M. Yashiro, T. Asahi, H. Masuhara, *J. Photochem. Photobiol. A* **2001**, *142*, 197 – 207.
[23] A. Vogel, J. Noack, G. Hüttman, G. Paltauf, *Appl. Phys. B* **2005**, *81*, 1015 – 1047.
[24] A. Takahara, N. Higashi, T. Kunitake, T. Kajiyama, *Macromolecules* **1988**, *21*, 2443 – 2446.
[25] C. D. Wagner, A. V. Naumkin, A. Kraut-Vass, J. W. Allison, C. J. Powell, J. R. Rumble, Jr., *NIST X-ray Photoelectron Spectroscopy Database: NIST Standard Reference Database 20*, Version 3.5, the National Institute of Standards and Technology (NIST), http://srdata.nist.gov/xps/.

Received: August 24, 2010
Published online on February 21, 2011

